

## Deactivation of Pt/wire-mesh and vanadia/monolith catalysts applied in selective catalytic reduction of NO<sub>x</sub> in flue gas

Morteza Sohrabi<sup>†</sup>, Farokhbag Moradi and Mehri Sanati\*

Department of Chemical Engineering, Amirkabir University of Technology, Tehran, Iran

\*School of Biosciences and Process Technology, Bioenergy Technology, Växjö University, SE-351, 95 Växjö, Sweden

(Received 26 August 2006 • accepted 18 December 2006)

**Abstract**—In this study the deactivation of Pt/wire mesh and vanadia/monolith catalysts by aerosol particles of some inorganic salts (K<sub>2</sub>SO<sub>4</sub>, KCl and ZnCl<sub>2</sub>) with high or low melting points has been investigated. The aerosol particles may either diffuse within the matrix of the catalysts and block the mezzo and micro pores, or deposit on the outer surface of the catalysts and form a porous layer causing a mass transfer resistance that ultimately deactivates the catalysts. It has been observed that in both Pt/wire mesh and vanadia/monolith catalysts the deactivation effect of ZnCl<sub>2</sub> was more pronounced compared to other salts. As an example, after 31 hours of exposure to ZnCl<sub>2</sub>, 10% of the catalysts activities was lost. This may be related to the ZnCl<sub>2</sub> lower melting point in comparison with other poisons. These results are in agreement with the previous findings for deactivation of wire-mesh catalysts used for oxidation of volatile organic compounds (VOC) and CO by exposing the catalysts to the aerosols generated from inorganic salts.

Key words: Vanadia/Monolith, Pt/Wire Mesh, SCR, Aerosol, Deactivation, Sub-micron Particles

### INTRODUCTION

In flue gases resulting from combustion of different fuels, especially biomass, various hazardous compounds such as NO<sub>x</sub>, CO and VOCs (volatile organic compounds) and fly ashes as sub-micron particles are present. It is known that nitrogen oxides (NO<sub>x</sub>) are amongst the most hazardous air pollutants. The present level of NO<sub>x</sub> emissions already poses a significant threat to human health and environment. There has been increasing public and government concern over the environmental impact of acid rain, to which nitrogen oxides contribute a substantial percentage [1]. The NO<sub>x</sub> formed from combustion of biomass, comprises approximately 40% of the total amount of gases that is emitted to the atmosphere [2].

There are different ways for removing NO<sub>x</sub> from the flue gas, among which primary control (combustion control) and secondary control (removing NO<sub>x</sub> from the flue gas) are the more important procedures [2]. The selective catalytic reduction (SCR) process is the most widely used technology for the control of NO<sub>x</sub> emission from stationary sources including power-plants and incinerators. This is largely due to the efficiency and selectivity of this method [3-5]. Three types of catalysts are normally used for such a purpose consisting of noble metals, base metals and zeolites [6-8]. SCR catalysts are usually mixtures of vanadium pentoxide and tungsten or molybdenum trioxide [5]. The V<sub>2</sub>O<sub>5</sub>/TiO<sub>2</sub> and vanadia-based catalysts have gained commercial approval for the SCR processes [9]. The overall reaction for NO reduction in the SCR process can be expressed as follows [10]:



Different types of catalysts, including monolith and wire mesh are

currently used for SCR reactions. Monolith catalysts consist of arrays of channels arranged either in cross-flow structures, or in parallel and approximately parallel structures. The support is covered with a thin and uniform catalytic layer which makes the internal diffusion resistance relatively low [11]. Owing to the low pressure drop, control of pollutants from mobile sources and nonautomotive catalytic systems is a major application of monolith catalysts [12]. These catalysts have been also applied to other processes such as CO<sub>2</sub> reforming of methane [13]. Wire-mesh catalysts have efficient mass and heat transfer performances but a relatively higher pressure drop.

Catalyst deactivation is a critical concern for many industries, which leads to the loss of catalytic activity and/or selectivity over time. This has a significant technical and economical impacts on the processes and affects the performance of a given reaction system or the economics of a certain chemical plant.

The catalysts applied in SCR reactions deactivate rapidly. The lifetime of the catalysts, having a significant role in the overall SCR system economics, is determined by the deactivation process [14]. Several mechanisms for the deactivation of SCR catalysts used for NO<sub>x</sub> decomposition have been put forward [9]. These may be classified as follows:

- (a) poisoning due to reactions on the surface of the catalyst,
- (b) blockage of micro and mezzo pore network as the result of formation of salts or deposition of fine particles on the surface of the catalyst (aerosol deposition),
- (c) masking of the catalyst surface by deposition of dust and thermal degradation,
- (d) decrease in the active phase of the catalysts due to erosion,
- (e) plugging of monolith catalysts by deposition of dust and larger particles.

Alkali metals are amongst the strongest poisons for V<sub>2</sub>O<sub>5</sub>/TiO<sub>2</sub>

<sup>†</sup>To whom correspondence should be addressed.

E-mail: sohrabi@aut.ac.ir

catalysts used for decomposition of NO [15]. The poisoning power of the salts is related to their basicity. The severity of poisoning follows the order of  $KCl > NaCl > K_2SO_4 > Na_2SO_4$ . Sulphur dioxide has a promoting effect on the activity due to the acidity improvement of the catalysts surface as the result of sulphate formation. Some studies have been carried out on the deactivating effects of alkali and alkali earth metals and some other compounds such as potassium, PbO,  $As_2O_3$ ,  $P_2O_5$ ,  $SO_2$ , HCl, chlorides and carbonaceous species [9,11,16-19].

Deactivation of environmental catalysts when applied in flue gas cleaning from biomass burning may be due to the deposition of fly ashes in the form of sub-micron particles. These are formed during combustion and subsequent cooling of the flue gas. The particles could deposit either on the surface of the catalysts or diffuse inside the pores. Certain studies have been carried out to recognize the nature and the size distribution of particles emitted during biomass combustion [20-23]. The results of elemental analysis revealed that the three most abundant elements were potassium, sulphur and chlorine. The size distributions of emitted particles usually follow a log-normal form. In an earlier study, mass elemental size distribution of the emitted aerosol was found to be in the range of 0.01-11  $\mu m$  [12]. Hegedus [24] studied the poisoning of porous catalysts when impure feed gases are used. The deactivation of a net type catalyst, exposed to the flue gas, was investigated by Berg et al. The results showed that the deactivation of catalyst started immediately after exposure to the flue gas [25].

In the present work, the procedure for preparing the deactivated samples of catalysts on a laboratory scale might be assumed to simulate the deactivation process in a real situation, i.e., in combustion systems when the SCR catalysts are exposed to the aerosol particles present in flue gases. It is obvious that the aerosol particles in such gases possess a poly-dispersed distribution. In this study, however, for the sake of simplicity the monodispersed aerosol particles of poison salts have been applied.

## EXPERIMENTAL

### 1. Aerosol Particles Generation and Characterization

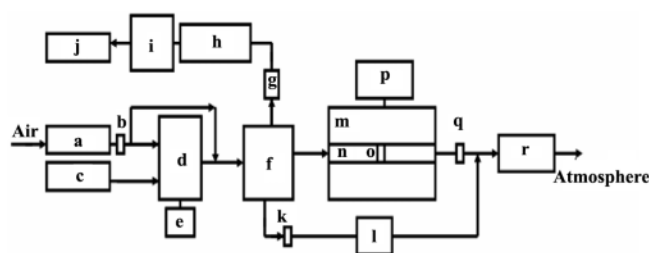


**Fig. 1. Schematic diagram of the deactivation system.**

- |                                   |                           |
|-----------------------------------|---------------------------|
| a. Air compressor                 | j. Personal computer      |
| b. Compressed air drier           | k. Air filter             |
| c. Syringe pump                   | l. Critical orifice       |
| d. Atomizer                       | m. Oven                   |
| e. Excess reservoir               | n. Deactivation chamber   |
| f. Dilution vessel                | o. Catalyst bed           |
| g. Aerosol dryer                  | p. Temperature controller |
| h. Differential mobility analyzer | q. Total filter           |
| i. Condensation particle counter  | r. Vacuum pump            |

The aerosol particle generation process is shown schematically in Fig. 1. A number of solutions containing 25  $g/dm^3$  of KCl,  $K_2SO_4$ , and  $ZnCl_2$  salts were prepared. The concentration of solutions plays an important role in the aerosol particle size formation. By increasing the concentration of solutions, the mean aerodynamic diameters of the particles are also increased. With such a concentration (25  $g/dm^3$ ), the count mean aerodynamic diameter (CMAD) of the aerosol particles is expected to be around 70 nm.

The aerosol particle generator was a Constant Output Atomizer (TSI, Model 3076). Compressed dry air was used to atomize the solution under a pressure of 2 bar. A Harvard 975 Mechanical Compact Syringe Pump with a 50  $cm^3$  syringe was used to direct the solution to the atomizer. The solution's flow rates were maintained at about 0.59  $cm^3/min$ . This is a critical flow rate [23], below which the generator output becomes unsteady, while at the higher values, the excess liquid is simply removed by impaction and drained off from the atomizer chamber to the reservoir vessel.

The number of particles is increased by increasing the pressure; however, the particle size is reduced. In atomized solutions, the small particles leave the system as aerosol particles (with geometric mean diameter less than 70 nm), whereas larger particles collide with the surface of the atomizer and settle down in the reservoir vessel. To reduce the relative humidity of the aerosol particles, the latter is mixed with compressed dry air. The excess air is used to dilute the flow and reduce the humidity of the aerosol particles. The aerosol particles number weighted size distribution was measured using a differential mobility spectrometer (Scanning Mobility Particle Sizer, (SMPS), TSI model 3934).

A flow of aerosol particles (0.3  $dm^3/min$ ) from the dilution vessel after passing a Nafion drier (Perma Pure Inc. US) passed through an aerosol physical characterization apparatus SMPS. This is a combination of a DMA (Differential Mobility Analyzer) and a CPC (Condensation Particle Counter). At the inlet of the DMA an impactor is installed to prevent the passage of larger particles through the apparatus. Aerosol particles are first classified in the DMA and then passed through a CPC (TSI model 3022A) which is a particle detector in the SMPS system. The upper limit of the aerosol particles concentration, counted in the CPC is 10000 particles/ $cm^3$ . The CPC was connected to a computer by which size distributions (mass, number and surface) and concentrations of the aerosol particles were evaluated.

Characterization of coarse particles (larger than 1  $\mu m$ ), was performed by using an Aerodynamic Particle Sizer (APS, TSI model 3320). The flow rate of aerosol particles through the instrument was 1  $dm^3/min$ . Further details of aerosol generation and characterization may be found elsewhere [26].

### 2. Deactivation Process

Deactivation tests have been carried out for Pt/wire mesh and vanadia/monolith catalysts in selective catalytic reduction of  $NO_x$ . Aerosol particles from the generator were mixed with dry compressed air and entered a dilution vessel having a volume of 2  $dm^3$ . Dry air was used to reduce the relative humidity of the flow containing aerosol particles. The dilution ratio in these experiments was kept around 0.72. By such a procedure, it was possible to adjust the relative humidity of the aerosol flow to less than 20% of that in the original stream. Aerosol particles leaving the dilution vessel were divided into three separate streams. The first with a flow rate of 0.3

dm<sup>3</sup>/min passed through SMPS. An impactor with a cut-off size of 805 nm was installed before the SMPS to prevent the entrance of larger particles through the system. The second, after passing through a total filter, was led through a critical orifice connected downstream to a vacuum pump. This was applied to reduce the flow rate of aerosol particles in the deactivation reactor in order to provide laminar flow. The third stream from the dilution vessel was introduced to the deactivation chamber. This was made of Pyrex glass, with a length of 100 cm and a diameter of 24 mm. For each deactivation test, the chamber was packed with six nets of the Pt/wire mesh and four channels of vanadia/monolith catalysts. The chamber was placed in an oven equipped with a panel having a temperature controller. The catalysts were deactivated by exposing to the generated aerosol particles of K<sub>2</sub>SO<sub>4</sub>, KCl and ZnCl<sub>2</sub> at 340 °C. The aerosol leaving the reactor was trapped in a filter to avoid environmental pollution. Each catalyst sample was exposed to the generated aerosol particles for 31 hours, before being subjected to the activity tests.

### 3. Activity Measurement

Deactivation patterns of both wire mesh and monolith catalysts were determined by first exposing the catalysts to the aerosol generated from different metal salts, followed by the measurement of activities of the partially poisoned catalysts in decomposition of NO<sub>x</sub> components. A schematic diagram of the experimental rig is shown in Fig. 2.

In this setup NO<sub>x</sub> gases (mixtures of NO and NO<sub>2</sub>) at 150 bar and 404 ppm concentration were supplied from a pressurized vessel with a flow rate of 4.2 dm<sup>3</sup>/min. Compressed dry air with a flow rate of 2.5 dm<sup>3</sup>/min was introduced to the NO<sub>x</sub> line. Ammonia (NH<sub>3</sub>) with a flow rate of 2 dm<sup>3</sup>/min was mixed with NO<sub>x</sub> line at the entrance part of the reactor. This was to prevent the formation of ammonium nitrate in the line. The reactor was made of stainless steel with internal diameter of 32 mm. Heating was provided by an electric protective heater compartment. The temperature of the reactor was controlled by a temperature controller device. In each experimental run the reactor was loaded with either six partially deactivated wire mesh nets or four channel monolith catalysts. The temperature range was between 200-450 °C.

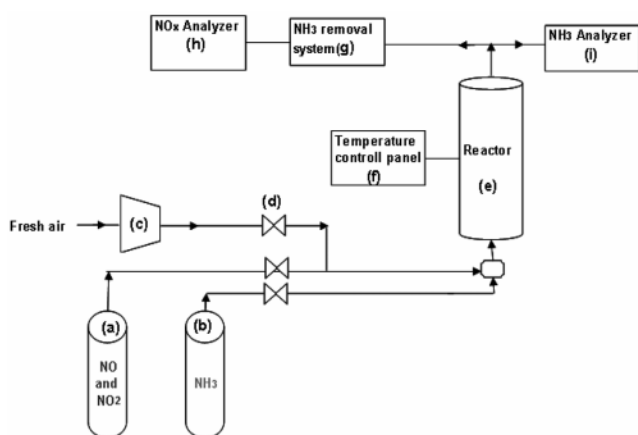


**Fig. 2. Schematic diagram of the activity measurement system.** (a) and (b) pressurized vessels, (c) air compressor, (d) control valve, (e) reactor, (f) temperature controller, (g) ammonia removal system, (h) NO<sub>x</sub> analyzer, (i) ammonia analyzer

The outlet of the reactor contains minor amounts of NH<sub>3</sub>, NO and NO<sub>2</sub>. The mixture was divided between two lines. The first was directed to an NH<sub>3</sub> detector (1302 Bruel & Kjar multi gas analyzer), while the second, after removing the ammonia from the gas stream by passing the latter through a diluted sulphuric acid solution, was led to an NO<sub>x</sub> analyzer. The NO<sub>x</sub> analyzer was an API model 200 chemiluminescence apparatus. To avoid possible corrosion caused by ammonia adsorption, all the tubing was made of Teflon.

### 4. Electron Microscopy

Scanning electron microscopy (SEM) of the fresh and deactivated samples was recorded with an electron micro probe analyzer (EMPA), model JEOL, JXA-8600. The microscope was equipped with an energy dispersive spectrometer (Tracor Northern model, series II) for preliminary investigation of point analysis and mapping of elements.

## RESULTS AND DISCUSSION

### 1. Monolith Catalyst

The vanadia/monolith catalyst was supplied by BASF. The catalyst samples treated by exposing to the aerosol generated from different inorganic salts were tested for their activities in decomposing of NO<sub>x</sub> compounds. The results are shown in Fig. 3. As it may be observed from this figure, in all cases, an increase in temperature from 200 to ca 350 °C enhances the conversion of NO<sub>x</sub>. However, decline in conversion occurs beyond this temperature. In addition,

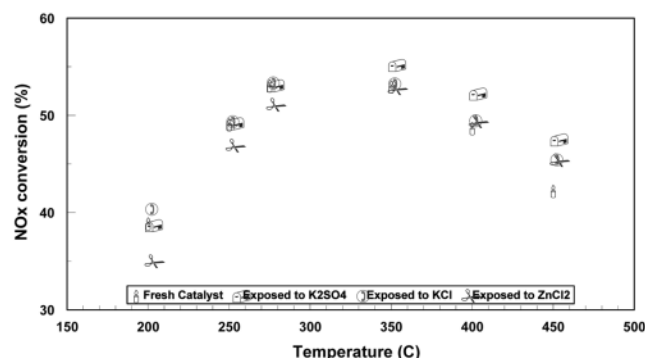


**Fig. 3. Effect of temperature on NO<sub>x</sub> decomposition with vanadia/monolith catalyst.**

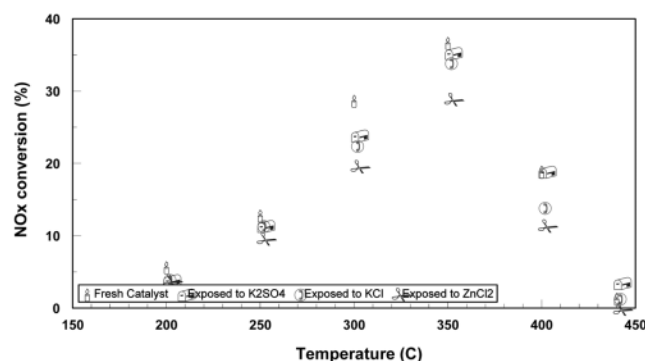


**Fig. 4. Effect of temperature on NO<sub>x</sub> decomposition with Pt/wire mesh catalyst.**

tion, it is clear that the deactivating effect of zinc chloride on vanadia/monolith catalyst is stronger than those generated from other salts.

## 2. Wire-mesh Catalyst

The Pt/wire mesh catalyst was supplied by Catator Company. The catalyst samples, prior to tests for their activities in reduction of  $\text{NO}_x$ , were exposed to aerosol generated from  $\text{K}_2\text{SO}_4$ ,  $\text{KCl}$  and  $\text{ZnCl}_2$ . In each experimental run six nets of catalysts were used. The results are shown in Fig. 4. Similar to the case observed for monolith catalyst, the  $\text{ZnCl}_2$  aerosol was found to have the strongest deactivating effect upon the wire mesh catalyst.

This could be related to a lower melting point of  $\text{ZnCl}_2$  in comparison with other salts and is discussed in the conclusion section.

## CONCLUSIONS

The results obtained from the present study show that the affinity of metal salts aerosols in deactivation of vanadia/monolith and Pt/wire mesh catalysts may be classified as  $\text{ZnCl}_2 > \text{KCl} > \text{K}_2\text{SO}_4$ . The deactivating effect of sub-micron particles could be due to the diffusion of the latter within the matrix of the catalyst and blockage of the mezzo and micro pores. The Electron microscopy revealed that both potassium salts and zinc chloride particles diffuse inside the catalyst; however, the depth of penetration of zinc chloride particles is more profound than that of potassium salts' particles (Figs.

5 and 6).

In the SEM pictures of the catalyst sample exposed to potassium chloride (Fig. 5) a distinct top layer with a thickness of approximately 2-4  $\mu\text{m}$  can be observed, while such a thickness for the catalyst exposed to zinc chloride is approximately 6-8  $\mu\text{m}$  (Fig. 6). The higher affinity of  $\text{ZnCl}_2$  in deactivating the catalysts lies on the lower melting point of this salt, i.e., 283 °C. Clearly at 340 °C,  $\text{ZnCl}_2$  is in either molten or gas states. Thus, the catalyst is in fact exposed to zinc chloride present in liquid or gas phases. One expects, therefore, to observe a higher penetration ability for  $\text{ZnCl}_2$  compared to that of potassium salts at this temperature.

It seems that the aerosols generated from the low melting point salts such as  $\text{ZnCl}_2$  present in the flue gases are the main sources of deactivation of environmental catalysts. Implementation of a cleaning system for elimination of sub-micron particles prior to passage of the flue gas through the catalysts bed is thus an effective method by which the catalysts lifetimes could be extended.

## REFERENCES

1. F. G. Medros, J. W. Eldridge and J. R. Kittrel, *Ind. Eng. Chem. Res.*, **28**, 1171 (1989).
2. H. Bosch and F. Janssen, *Catalysis Today*, **2**, 342 (1987).
3. H. Bosch and F. Janssen, *Catal. Today*, **2**, 369 (1989).
4. L. Lietti and P. Forzatti, *Heter. Chem. Rev.*, **3**, 33 (1996).
5. P. Forzatti, I. Nova and A. Beretta, *Catalysis Today*, **56**, 431 (2000).
6. A. Bell and L. E. Manzer, *Chem. Eng. Prog.*, **91**(2), (1995).
7. H. T. Lee and H. K. Rhee, *Korean J. Chem. Eng.*, **19**, 574 (2002).
8. H. K. Seo, J. W. Oh, S. C. Lee, J. Y. Sung and S. J. Choung, *Korean J. Chem. Eng.*, **18**, 698 (2001).
9. J. P. Chen, M. A. Buzanowski, R. T. Yang and J. E. Cichanowicz, *J. Air Waste Manage. Association*, **40**, 1403 (1990).
10. J. W. Beekman and L. L. Hegedus, *Ind. Eng. Chem. Res.*, **30**, 969 (1991).
11. A. Cybulski and J. A. Moulijn, J. A., *Catal. Rev-Sci. Eng.*, **36**, 179 (1994).
12. G. Özkan and A. Gülşendoğu, *Ind. Eng. Chem. Res.*, **36**, 4734 (1997).
13. S. J. Kong, J. H. Jun and K. J. Yoon, *Korean J. Chem. Eng.*, **21**, 793 (2004).
14. R. Khodayari and C. U. Ingemar Odenbrand, *Chem. Eng. Sci.*, **54**, 1775 (1999).
15. J. P. Chen and R. T. Yang, *Journal of Catalysis*, **125**, 411 (1990).
16. Babcock Hitachi Company, Commercial Information (1990).
17. K. Suikannen, PhD Thesis, Dept. of Chem. Eng., Lappeenranta University of Technology (1999).
18. S. Srihiranpullopp, P. Praserttham and T. Mongkhonsi, *Korean J. Chem. Eng.*, **17**, 548 (2000).
19. R. Khodayary and C. U. Ingemar Odenbrand, *Ind. Eng. Chem. Res.*, **37**, 1196 (1998).
20. J. Pagels, M. Strand, A. Gudmundsson, A. Szpila, J. Rissler, E. Swietlicki, M. Sanati and M. Bohgard, *Proceedings of the european aerosol conference*, Leipzig, September 3-7 (2001).
21. K. A. Christensen, PhD Thesis, University of Copenhagen, Denmark (1995).
22. T. Vamari, E. I. Kauppinen, J. Kurkela, J. K. Jokiniemi, G. Sfiris and H. J. Revitzer, *J. Aerosol Sci.*, **29**, 445 (1998).

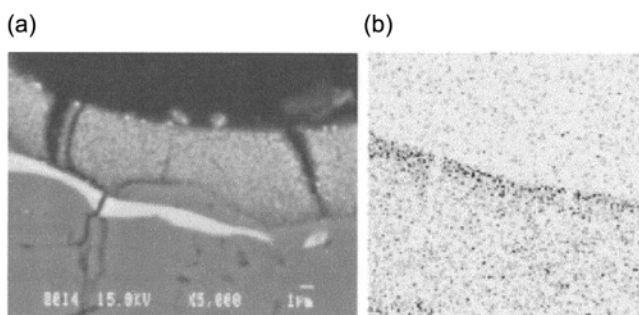


**Fig. 5. Cross section and X-ray mapping of KCl deactivated sample of Pt/wire mesh catalyst.**

(a) cross section of the sample exposed to  $\text{KCl}$ ; (b) X-ray mapping of potassium in the sample

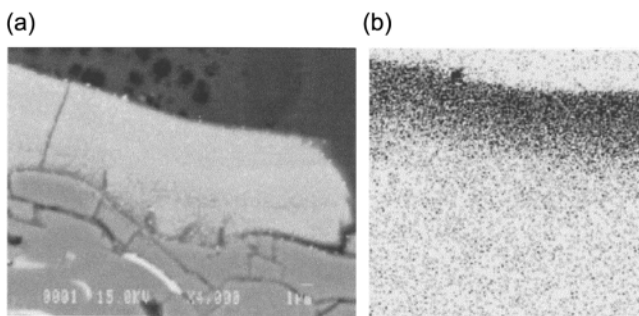


**Fig. 6. Cross section and mapping of  $\text{ZnCl}_2$  deactivated sample of Pt/wire mesh catalyst.**

(a) cross section of the sample exposed to  $\text{ZnCl}_2$ ; (b) X-ray mapping of zinc in the sample

23. E. I. Kauppinen and T. A. Pakkanen, *Environ. Sci. Technol.*, **24**, 1811 (1990).
24. L. L. Hegedus, *Ind. Eng. Chem. Fundamentals*, **13**, 3 (1974).
25. M. Berg, T. Hargitai, J. Brandin and N. Berg, *Progress in thermo-chemical biomass conversion*, Bridgewater, A. V., editor, Blackwell Scientific Publications, UK (2001).
26. F. Moradi, PhD Thesis, Amirkabir University of Technology, Tehran, Iran (2003).